Available online at www.sciencedirect.com

ScienceDirect

Journal of Exercise Science & Fitness 12 (2014) 88–95

www.elsevier.com/locate/jesf

Original article

Diastolic function alteration mechanisms in physiologic hypertrophy versus pathologic hypertrophy are elucidated by model-based Doppler E-wave analysis

Simeng Zhu [a], Thomas Morrell [a], Astrid Apor [b], Béla Merkely [b], Hajnalka Vágó [b], Attila Tóth [b], Erina Ghosh [c], Sándor J. Kovács [c,d,*]

[a] *Washington University Compton Scholars Program, Cardiovascular Biophysics Laboratory, Cardiovascular Division, School of Medicine, Washington University, St. Louis, MO, USA*

[b] *Heart Center, Semmelweis University, Budapest, Hungary*

[c] *Department of Biomedical Engineering, School of Engineering and Applied Science, Washington University, St. Louis, MO, USA*

[d] *Department of Internal Medicine, School of Medicine, Washington University, St. Louis, MO, USA*

Received 22 March 2014; revised 28 July 2014; accepted 9 October 2014
Available online 12 November 2014

Abstract

Athletic training can result in increased left ventricular (LV) wall thickness, termed *physiologic hypertrophy* (PhH). By contrast, pathologic hypertrophy (PaH) can be due to hypertension, aortic stenosis, or genetic mutation causing hypertrophic cardiomyopathy (HCM). Because morphologic (LV dimension, wall thickness, mass, etc.) and functional index similarities (LV ejection fraction, cardiac output, peak filling rate, etc.) limit diagnostic specificity, ability to differentiate between PhH and PaH is important. Conventional echocardiographic diastolic function (DF) indexes have limited ability to differentiate between PhH and PaH and cannot provide information on chamber property (stiffness and relaxation). We hypothesized that kinematic model-based DF assessment can differentiate between PhH and PaH and, by providing chamber properties, has even greater value compared with conventional metrics. For validation, we assessed DF in the following three age-matched groups: pathologic (HCM) hypertrophy (PaH, $n = 14$), PhH (Olympic rowers, PhH, $n = 21$), and controls ($n = 21$). Magnetic resonance imaging confirmed presence of both types of hypertrophy and determined LV mass and chamber size. Model-based indexes, chamber stiffness (k), relaxation/viscoelasticity (c), and load (x_o) and conventional indexes, E_{peak} (peak of E-wave), ratio of E_{peak} to A_{peak} (E/A), E-wave acceleration time (AT), and E-wave deceleration time (DT) were computed. We analyzed 1588 E waves distributed as follows: 328 (PaH), 672 (athletes), and 588 (controls). Among conventional indexes, E_{peak} and E-wave DT were similar between PaH and PhH, whereas E/A and E-wave AT were lower in PaH. Model-based analysis showed that PaH had significantly higher relaxation/viscoelasticity (c) and chamber stiffness (k) than PhH. The physiologic equation of motion for filling-based derivation of the model provides a mechanistic understanding of the differences between PhH and PaH.

Keywords: Diastolic function; Echocardiography; Pathologic hypertrophy; Physiologic hypertrophy

Introduction

Hypertrophic cardiomyopathy (HCM) is caused by mutation in genes encoding cardiac sarcomere proteins. It is a common genetic disorder of the cardiovascular system characterized by left ventricular (LV) wall thickening without

* Corresponding author. Cardiovascular Biophysics Laboratory, Washington University School of Medicine, 660 South Euclid Avenue, Box 8086, St. Louis, MO 63110, USA.

E-mail address: sjk@wuphys.wustl.edu (S.J. Kovács).

http://dx.doi.org/10.1016/j.jesf.2014.10.001

chamber dilation.[1,2] It can cause sudden death in asymptomatic patients or progressive heart failure.[3] HCM is an example of pathologic hypertrophy (PaH). By contrast, physiologic hypertrophy (PhH) is induced by exercise, pregnancy, or normal growth.[4,5] Although athletic training can change the heart morphologically (LV mass, dimension, shape, etc.) and functionally [LV ejection fraction (LVEF), stroke volume, peak filling rate, heart rate, etc.], it can be difficult to differentiate PaH from PhH. The ability to differentiate is important, because undetected HCM is the most frequent cause of sudden death of athletes during exercise, and misdiagnosis of HCM can lead to unnecessary disqualification of athletes.[6] Electrocardiography is unable to differentiate PaH from PhH.[7]

PaH and PhH manifest differences in cardiac function, which can be evaluated by echocardiography. Previous studies have used two-dimensional echocardiography,[2] ultrasound speckle tracking,[8] tissue Doppler imaging,[9–12] transmitral flow,[13] and M-mode echocardiography[14] to show differences in diastolic function (DF). Transmitral flow analysis has demonstrated limited value in differentiating between PaH and PhH.[6,14] Common DF indexes, including the ratio of peak early transmitral flow to peak late atrial filling (E/A), E_{peak} (peak E-wave velocity in centimeter/second), E-wave acceleration time (AT in milliseconds), and E-wave deceleration time (DT in milliseconds),[15] have provided inconsistent results regarding DF at rest. Moreover, E-wave parameters are load dependent and have not been derived from basic physiologic principles that govern filling.[15–21] Indexes (such as E/A) are generated by the complex interplay of simultaneous physiologic determinants and chamber properties. Specifically, E-wave DT has been shown to explicitly depend on both chamber stiffness and chamber relaxation/viscoelasticity.[22]

To overcome the limitations of conventional indexes, we quantified DF using a previously validated mechanistic model of filling that incorporates the mechanical suction-pump attribute of the LV. Accordingly, we analyzed E-waves using the parametrized diastolic filling (PDF) formalism (Appendix A).[23] We have previously characterized PhH of the athlete heart and compared it with the heart of age-matched controls in terms of PDF-derived indexes and chamber properties.[24] We found significant differences in stiffness and load between Olympic athletes and controls. Here, we use our previous work as a foundation to test the hypothesis that PDF formalism-derived chamber properties can differentiate PaH from PhH. By performing serial echocardiographic assessments of DF, model-based analysis of transmitral flow may elucidate and characterize the mechanistic changes in HCM compared with athletes and controls.

Methods

Patient selection

We analyzed data from 14 HCM patients, 21 athletes, and 21 healthy controls. All three groups were matched for age, sex, and body surface area (BSA; Table 1). The 14 patients (average age: 31 years; 11 men) with clinically established diagnosis of HCM from the cardiomyopathy clinic at Semmelweis University Heart Center (Budapest Hungary) were recruited and screened for magnetic resonance imaging (MRI) compatibility. Three of the 14 patients were not on any medication. The classes of medications for the remaining 11 patients were as follows: 10 on beta-blockers, three on calcium-channel blockers, three on angiotensin-converting

Table 1
Clinical descriptors.

Parameter	Controls (n = 21)	PhH (n = 21)	PaH (n = 14)	PhH vs. controls	PaH vs. controls	PhH vs. PaH
Clinical attributes						
Age, y	30 ± 5	27 ± 9	31 ± 14	0.588	0.865	0.350
Height, cm	180 ± 7	182 ± 9	173 ± 6	0.965	0.019	0.011
Weight, kg	80 ± 12	77 ± 12	84 ± 15	0.830	0.644	0.339
BSA, m^2	2.0 ± 0.2	2.0 ± 0.2	2.0 ± 0.2	0.898	0.973	0.984
HR, beats/min	67 ± 9	57 ± 11	63 ± 7	0.003	0.361	0.200
Systolic BP, mmHg	141 ± 13	143 ± 14	133 ± 21	0.577	0.665	0.145
Diastolic BP, mmHg	85 ± 10	75 ± 13	78 ± 9	0.034	0.244	0.717
LV dimension and mass-derived indexes						
LVEDV, mL	192 ± 25	228 ± 52	182 ± 34	0.010	0.941	0.006
LVEDV index, mL/m^2 [a]	95 ± 14	115 ± 19	91 ± 15	<0.001	0.955	<0.001
LVESV, mL	79 ± 18	93 ± 29	62 ± 16	0.024	0.343	<0.001
LVESV index, mL/m^2 [a]	40 ± 8	47 ± 12	31 ± 7	0.015	0.154	<0.001
LVSV, mL	115 ± 15	134 ± 27	120 ± 29	0.039	0.754	0.245
LVSV index, mL/m^2 [a]	58 ± 5	68 ± 11	60 ± 13	0.010	0.778	0.089
LV mass, g	132 ± 20	171 ± 42	228 ± 65	0.028	<0.001	0.002
LV mass index, mL/m^2 [a]	66 ± 8	86 ± 17	115 ± 31	0.013	<0.001	<0.001
LVWT, mm	10 ± 1	13 ± 2	26 ± 5	0.107	<0.001	<0.001
LVEF, %	59 ± 6	60 ± 5	66 ± 7	0.869	0.049	0.011
Cardiac output, L/min	7.7 ± 1.5	7.5 ± 1.5	7.6 ± 1.6	0.874	0.976	0.967

BP = blood pressure; BSA = body surface area; HR = heart rate; LVEDV = left ventricular end-diastolic volume; LVEF = left ventricular ejection fraction; LVESV = left ventricular end-systolic volume; LVSV = left ventricular stroke volume; LVWT = left ventricular average wall thickness; PaH = pathologic hypertrophy; PhH = physiologic hypertrophy.

[a] These parameters are normalized to BSA. Data are presented as mean ± standard deviation.

enzyme inhibitors, one on anticoagulants, one on antiarrhythmic drugs, and one on mineralocorticoids. All the athletes were involved in endurance sport (mainly canoeing). The controls were healthy individuals who were either university students or employees, none of whom participated in competitive sports. All of the participants provided written informed consent for participation in the study in accordance with the Medical Research Council Scientific and Ethical Committee criteria (Semmelweis University).

Echocardiography

A complete echocardiographic examination was performed on all patients in accordance with the American Society of Echocardiography criteria with a standard clinical imaging system (Philips iE33; Philips Healthcare, Andover, MA, USA).[25] The wall filter was set at 125 Hz. Two-dimensional images in apical two- and four-chamber views were obtained. Pulsed Doppler was used in the apical four-chamber view for transmitral Doppler with the 4-mm sample volume located at the leaflet tips and with patients in the left lateral decubitus position. A standardized method of passive leg elevation in the recumbent position was used with 0°, 45°, and 90° foam wedges to generate physiologic load variation during E-wave recording.

Echocardiographic data analysis

The total number of E-waves analyzed conventionally (E-waves approximated as triangles) and through the PDF formalism was 1558: 328 from HCM, 672 from athletes, and 588 from controls. Only beats with clear contours were selected, digitized, and cropped using a custom MATLAB (MathWorks, Natick, MA, USA) program. The E_{peak}, E-wave AT, E-wave DT, peak A-wave velocity, E/A, and heart rates were computed. The PDF parameters were computed from E-waves as previously described (Appendix A).[26] In brief, the digitized E-wave image was used to determine the maximum velocity envelope, from which an automated PDF fit is obtained using the Levenberg–Marquardt algorithm. The output includes a measure of goodness of fit and an explicit measurement of error. Fitting generates three (mathematically unique) PDF parameters (c, k, and x_o) for each E wave (Fig. 1). In addition, peak atrioventricular (AV) pressure gradient kx_o, maximum resistive force opposing filling cE_{peak}, and stored elastic strain energy before valve opening $1/2kx_o^2$ were also computed.

Cardiac MRI

The MRI examination (Achieva 1.5T Dual Nova HP R2.6.3p7, cardiac coil; Philips Healthcare, Andover, MA, USA) used "breath hold" at end-expiration for each image acquisition to eliminate respiratory motion artifact. After obtaining scout images, steady-state free-precession breath-hold cine images were acquired in four-, three-, and two-chamber long-axis planes and in sequential 8-mm short-axis slices (flip angle 60°, 0-mm gap) from the AV ring to the apex. The height and weight of each participant provided the BSA through the Mosteller formula.[27]

MRI data analysis

The LV end-diastolic volume, LV end-systolic volume, LV stroke volume, LV mass, and their BSA-normalized values were computed. The LV average (maximal) wall thickness and LVEF were determined using standard methods. The LV volume, LVEF, and mass were quantified using planimetry of end-diastolic and end-systolic short-axis balanced steady-state free-precession cine images with QMass 7.1 analysis software (Magnetic Resonance Analytical Software System; Medis Medical Imaging Systems, Leiden, The Netherlands). Cardiac output was calculated by multiplying heart rate by stroke volume. These parameters are listed in Table 1.

Statistical analyses

Conventional and PDF parameters for all E-waves in each individual were averaged. Mean patient values were used to calculate group averages (Table 2) and to determine statistical significance. The MRI data were also averaged for each group and are reported in Table 1. One-way analysis of variance with a Tukey *post hoc* test was performed in SPSS Statistics 22 (IBM, Armonk, NY, USA) to determine whether the parameter value difference between groups was significant, using $p < 0.05$ as the criterion.

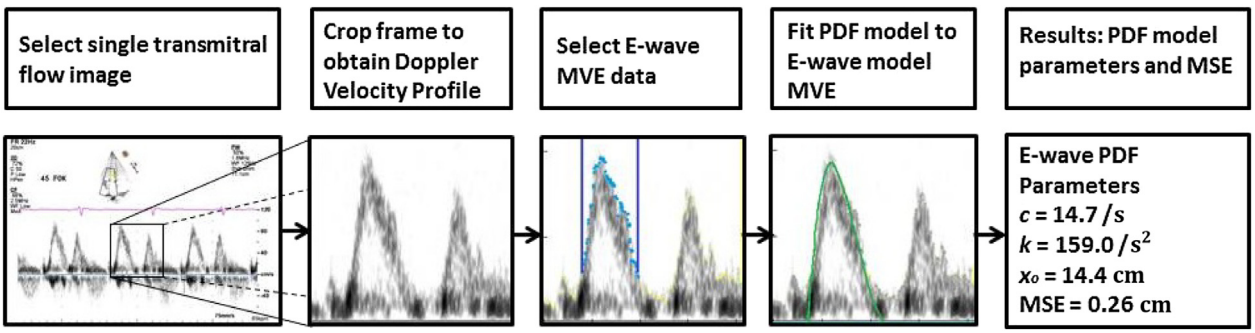

Fig. 1. Sequence of operational steps for computing PDF parameters from clinical echocardiographic E-wave contours (blue dots denote MVE used as input to the model). The PDF model output consists of the mathematically unique parameters (x_o, c, and k) that specify each E wave. The PDF model-predicted fit is shown as the green contour. MVE = maximum velocity envelope; MSE = mean square error (see text for details); PDF = parametrized diastolic filling.

Table 2
Transmitral flow measurement.

Parameter	Controls ($n = 21$)	PhH ($n = 21$)	PaH ($n = 14$)	PhH vs. controls	PaH vs. controls	PhH vs. PaH
Conventional Doppler indexes						
E_{peak}, cm/s	78 ± 14	84 ± 16	91 ± 23	0.527	0.095	0.487
E-wave AT, ms	80 ± 6	112 ± 16	75 ± 6	<0.001	0.446	<0.001
E-wave DT, ms	162 ± 23	220 ± 32	203 ± 66	<0.001	0.019	0.421
E_{dur}, ms	279 ± 32	332 ± 42	297 ± 37	<0.001	0.358	0.023
VTI, m	0.108 ± 0.016	0.139 ± 0.028	0.131 ± 0.043	0.028	0.076	0.808
E/A	1.7 ± 0.4	1.9 ± 0.5	1.5 ± 0.4	0.193	0.548	0.030
PDF parameters and indexes computed from them						
c, g/s	15.4 ± 2.6	15.0 ± 3.1	19.3 ± 2.9	0.905	<0.001	<0.001
k, g/s^2	235 ± 31	188 ± 44	248 ± 45	<0.001	0.619	<0.001
x_o, cm	9.3 ± 1.4	11.8 ± 2.5	12.0 ± 4.2	0.011	0.017	0.987
c^2-4mk, g^2/s^2	−687 ± 115	−492 ± 153	−603 ± 194	<0.001	0.253	0.099
$1/2kx_o^2$, mJ	1.1 ± 0.4	1.4 ± 0.7	1.9 ± 1.6	0.519	0.028	0.227
kx_o, N	21.9 ± 4.8	21.9 ± 6.3	28.9 ± 8.3	0.998	0.007	0.007
cE_{peak}, N	11.9 ± 3.0	12.6 ± 4.3	17.6 ± 6.1	0.859	<0.001	0.005
M	1.09 ± 0.12	1.08 ± 0.16	1.18 ± 0.11	0.993	0.134	0.109

$1/2kx_o^2$ = kinetic energy; AT = acceleration time; c = relaxation/viscoelasticity; cE_{peak} = peak resistive force; DT = deceleration time; E/A = ratio of E-wave peak to A-wave peak; E_{dur} = duration of E wave; E_{peak} = peak velocity of E wave; k = chamber stiffness; kx_o = peak atrioventricular pressure gradient; M = load-independent index of diastolic filling; PaH = pathologic hypertrophy; PDF = parametrized diastolic filling; PhH = physiologic hypertrophy; VTI = velocity time integral, the area under the E-wave; x_o = load.

Results

Characteristics of the HCM, athlete, and control groups

Table 1 provides the clinical descriptors of the study cohort ($n = 56$). The sex of the participants is as follows: 11 men/three women in the HCM group, 18 men/three women athletes, and 19 men/two women in the control group. All athletes participated in endurance training (canoeing), with 16 of the 21 being elite athletes and the remaining five being master athletes. Among the elite athletes, 11 were members of the Hungarian national team, two were Olympic athletes, and three were world champions. The control group consisted of healthy university students or university employees, none of whom participated in competitive sports.

Comparison between the athlete and control groups has been previously reported by our group.[24] The PaH group did not differ from athletes and controls in age, weight, BSA, heart rate, cardiac output, and systolic/diastolic blood pressure (Table 1).

The LV chamber dimensions and mass were determined from MRI data. The LV cavity size of the HCM group was significantly lower than athletes but comparable to controls, except for the BSA-normalized LV volume index at end systole (Table 1). The stroke volume of the HCM group was slightly lower than athletes but similar to controls (Table 1); however, LVEF (66 ± 7%) of the HCM group was significantly higher than athletes (60 ± 5%; $p = 0.011$) and controls (59 ± 6%; $p = 0.049$). The HCM group had substantially higher LV mass (228 ± 65 g) than athletes (171 ± 42 g; $p = 0.002$) and controls (132 ± 20 g; $p < 0.001$). As required by the criterion for diagnosing HCM (i.e., LV wall thickness ≥ 15 mm), the LV wall thickness of patients in the HCM group (26 ± 5 mm) was markedly higher than in athletes (13 ± 2 mm; $p < 0.001$) and in controls (10 ± 1 mm; $p < 0.001$). These attributes (dimension, mass, and wall thickness) confirm the presence of PaH in the HCM group.

DF assessment from transmitral flow: conventional and PDF parameters

The conventional Doppler echocardiographic and PDF parameters are shown in Table 2. The E_{peak} in PaH is comparable to the other groups. The E/A (1.5 ± 0.4) in PaH is significantly lower than athletes (1.9 ± 0.5; $p = 0.030$) but similar to controls (1.7 ± 0.4; $p = 0.548$). The E_{dur} in PaH (297 ± 37 ms) is significantly lower than in athletes (332 ± 42 ms; $p = 0.023$) and comparable with controls (279 ± 32 ms). The PaH group's E-wave DT (203 ± 66 ms) is comparable with the athlete group but markedly longer than controls (162 ± 23 ms; $p = 0.019$). The conventional echocardiographic measurements are in accordance with previous studies.[9,28]

The PDF parameter-based comparison revealed distinctive features of each type of hypertrophy. Fig. 2 shows three representative E waves, one from each group, along with their PDF parameters. Compared with controls, both PaH patients and athletes had substantially elevated but indistinguishable preloads (x_o: 12.0 ± 4.2 cm in PaH; 11.8 ± 2.5 cm in athletes; and 9.3 ± 1.4 cm in controls). Relaxation/viscoelasticity was increased only in PaH patients but not in athletes (c: 19.3 ± 2.9 g/s in PaH; 15.0 ± 3.1 g/s in athletes; and 15.4 ± 2.6 g/s in controls). Compared with controls, LV chamber stiffness was elevated in PaH patients but was significantly lower in athletes (k: 248 ± 45 g/s^2 in PaH; 188 ± 44 g/s^2 in athletes; and 235 ± 31 g/s^2 in controls). E-wave area (the velocity time integral or VTI) was comparable between athletes (0.139 ± 0.03 m) and PaH patients (0.131 ± 0.04 m) and higher than the control group (0.108 ± 0.02 m). The peak recoil force (kx_o) and peak

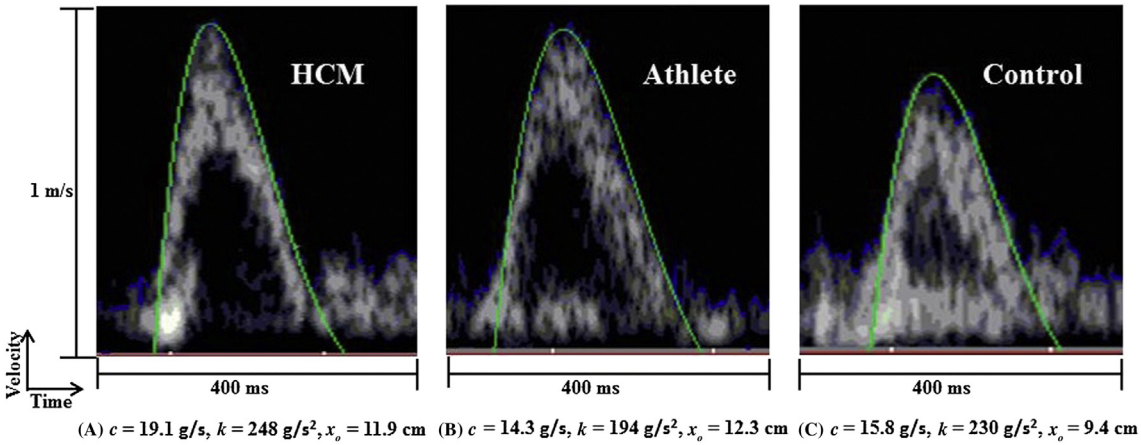

Fig. 2. Three E-waves with values of their PDF parameters. (A) Pathologic hypertrophy (HCM); (B) physiologic hypertrophy (rowing athlete); (C) Control. HCM = hypertrophic cardiomyopathy; PDF = parametrized diastolic filling.

resistive force (cE_{peak}) were significantly higher in the PaH group than in the other two groups (Table 2). We also calculated M, the load-independent index of DF.[29] We found M to be similar across the three groups (1.18 ± 0.11 in HCM; 0.108 ± 0.16 in athletes; and 1.09 ± 0.12 in controls).

Discussion

The morphologic similarity between PaH and PhH makes differentiation difficult. The common clinical diagnostic criterion for PaH is LV wall thickness of 15 mm or more in the absence of other factors that may cause LV hypertrophy.[7] Meanwhile, exercise typically remodels the LV such that its wall thickness would mildly increase, up to 12 mm.[6] This leaves a "gray zone" where the wall thickness falls between 13 and 15 mm, which could be due to either exercise or mild PaH.[6] From a functional perspective, athlete hearts at rest have similar echocardiographic parameters as control patients.[24] When compared with PaH patients, athletes have normal E/A, whereas PaH patients have abnormal filling and tissue Doppler patterns.[30] However, conventional echocardiographic parameters are empirical and provide no mechanistic information. To overcome this, we used the PDF formalism to assess DF by analyzing E-waves in athletes, PaH patients, and controls. We sought to elucidate and characterize differences in diastolic chamber (kinematic) properties among these groups. We found that chamber properties were significantly different between groups. Many previous studies have analyzed transmitral flow to assess DF using mainly E/A, which was found to be significantly smaller in PaH patients than in PhH (athletes).[6,13] Moreover, it has been repeatedly shown that LV relaxation in PaH patients is significantly delayed.[9,31,32]

Distinguishing power of PDF formalism

The PDF formalism incorporates the suction-pump attribute of the LV. Filling is modeled by Newton's Second Law in analogy to the motion of a previously displaced, damped, harmonic oscillator that recoils from rest. Therefore, the velocity is characterized by the following three parameters: chamber stiffness k, chamber viscoelasticity/relaxation c, and volumetric preload x_o. These parameters uniquely characterize each E wave in terms of the chamber's physiologic attributes. Although conventional parameters such as E-wave DT have been shown to correlate with and be attributed solely to stiffness,[33] more detailed analysis has revealed that E-wave DT is jointly determined by stiffness and relaxation/viscoelasticity (k and c) rather than stiffness alone (k).[22] Therefore, PDF analysis allows characterization of DF with greater specificity. The PDF formalism has been applied in multiple clinical settings (diabetes, hypertension, heart failure, caloric restriction) where conventional methods demonstrated limited utility or were unable to differentiate between groups.[34–37]

Trends in conventional echocardiographic indexes

Doppler E- and A-waves were analyzed conventionally, by approximating waveforms as triangles. We computed E_{peak}, E-wave AT and E-wave DT, and E/A in 1588 cycles from the three groups. We found that both athletes and PaH patients had longer E-wave DT compared with controls. E-wave duration was longest in athletes and it was significantly higher than in PaH patients. E_{peak} was not significantly different between the three groups. However, E/A was highest in athletes and was statistically significantly higher than in PaH patients. The E-VTI was similar in athletes and PaH patients but it was higher than controls.

Combined with the LV dimension information in Table 1, these results indicate that at rest, the athlete heart aspirates a larger volume per beat than the PaH heart, although the difference is not statistically significant. Moreover, because the resting heart rates of athletes are lower than PaH patients (statistically not significant), the cardiac output of pathologic and physiologic hypertrophic hearts remains indistinguishable. Therefore, these conventional echocardiographic flow and dimension-based indexes are unable to differentiate between PaH and PhH.

Trends in PDF-based indexes

Considering the PDF parameters, we found that c was higher (worse relaxation) in PaH patients than in athletes. The value of c was also higher in PaH patients than in controls. Athlete hearts had the lowest stiffness (k) among the three groups. The stiffness in controls and PaH hearts was comparable. The volumetric preload (x_o) was comparable in athletes and PaH patients and it was significantly higher than in controls. Therefore, the PDF parameters c and k can differentiate between PaH and PhH.

The initial maximum recoil force (kx_o; peak instantaneous AV pressure gradient analog[38]) was much higher in PaH than PhH due to the higher stiffness (k) in these chambers. Therefore, PaH patients have to generate a greater AV pressure gradient (proportional to recoil force[38]) to fill with a volume similar to that of the athlete heart. The peak resistive force (cE_{peak}) was also higher in PaH patients compared with controls and athletes, indicating a higher resistance (impaired relaxation) to filling in these hearts. The load-independent index of DF, M, is a dimensionless parameter defined by the ratio of peak recoil force to peak resistive force. M was significantly higher (worse) in PaH patients. This indicates that, for a given increase in the peak resistive force, the peak recoil force would increase by a greater amount in PaH patients, indicating a lower filling efficiency compared with PhH or controls.

Physiologic and clinical interpretation of results

By analyzing E-waves through the PDF formalism, we found that diastolic dysfunction in PaH patients is characterized by higher chamber stiffness (higher k) and by delayed relaxation (higher c). Increased stiffness means that when filling by the same incremental volume, the pressure increase (dP/dV) in PaH patients is greater than in PhH. In response to exercise, which requires increased filling volume, the chamber with PhH can increase its filling volume with a lower increase in pressure compared with PaH as a result of better relaxation. A higher value for the relaxation/viscoelasticity parameter c indicates delayed or incomplete relaxation (residual diastolic tone) and higher diastolic pressures. In concordance with results reported from other PaH studies using invasive methods,[32,39,40] increased c and k values accurately reflect the physiology. According to Gwathmey et al, the cause of delayed relaxation in PaH is cytosolic Ca^{2+} overload.[31] Delayed sequestration of Ca^{2+} into the sarcoplasmic reticulum implies incomplete crossbridge detachment and increased residual diastolic tone.[41] The higher chamber stiffness in PaH is the combined effect of increased LV mass, decreased LV chamber volume, and elevated myocardial stiffness.[32]

Although the average volumetric preload (x_o)—a determinant of E_{peak}—is comparable between the two groups at rest, meaning that both types of chambers aspirate about the same amount of blood with each E wave, PaH chambers generate a much higher peak AV pressure gradient (kx_o) than athletes to achieve it. This provides a mechanistic explanation, not obtainable from conventional E-wave-derived metrics, of how this form of diastolic dysfunction results in inefficient filling in PaH. It reinforces the view that diastolic dysfunction can be viewed as a state of impedance mismatch.[42] In addition, the higher maximum resistive force opposing filling (cE_{peak}) in PaH conveys a similar message.

Limitations

In identifying chamber property differences in PhH versus PaH, we did not further quantify differences among PhH individuals due to strength training versus endurance training versus combination training. In addition, the modest sample size for each group limited our ability to derive definitive parameter value ranges. While sex-based differences have been reported, our sample size did not permit us to make any sex-based conclusions. All of these limitations are mitigated to an acceptable degree by the large sample of E-waves analyzed ($n = 1588$). In addition, because age is a known DF determinant, basing the analysis on three age-matched groups reinforces our conclusions. Although some studies found fat-free mass to be a better scaling factor than BSA in comparing cardiac dimensions,[43,44] due to lack of data on fat-free mass, BSA was used instead.

Conclusion

The morphologic similarities between PhH and PaH can make echocardiographic differentiation a challenge. Even if some conventional indexes can differentiate between groups, their physiologic interpretation remains unclear. To overcome these limitations, we analyzed DF using conventional and PDF formalism-derived indexes. Our approach differentiated between the PaH and PhH and control groups characterized by MRI and echocardiography, when conventional indexes failed to do so. Importantly, our method elucidated the group-differentiating role of stiffness and relaxation as chamber properties. Because stiffness increases E_{peak} and impaired relaxation decreases E_{peak}, our model-based approach explicitly delineates the extent to which stiffness and relaxation are altered and provides a mechanistic explanation as to why conventional indexes, E_{peak} and E-wave DT, are unable to differentiate between groups.

Conflicts of interest

All contributing authors declare no conflicts of interest.

Acknowledgments

This work was supported in part by the Alan A. and Edith L. Wolff Charitable Trust (St. Louis, MO, USA) and the Barnes-Jewish Hospital Foundation (#6749-33). E.G. is the recipient of a Heartland Affiliate predoctoral fellowship award (11PRE4950009) from the American Heart Association. T.M. and S.Z. are recipients of Honorary Scholars Summer Research Grants from Washington University in Saint Louis (MO, USA).

Appendix A. The parametrized diastolic filling formalism

The parametrized diastolic filling (PDF) formalism characterizes suction-initiated transmitral flow in analogy to the motion (kinematics) of a previously displaced, damped, harmonic oscillator that recoils from rest. This method applies Newton's Second Law and predicts E-wave (transmitral flow velocity) contours parametrized in terms of chamber stiffness, relaxation/viscoelasticity, and load. Accordingly, per unit mass, the recoil process is governed by Newton's Second Law of motion.

$$d^2x/dt^2 + cdx/dt + kx = 0 \quad (1)$$

where c and k represent damping (viscoelasticity/relaxation) and ventricular stiffness (spring constant), respectively. The oscillator spring has been displaced by x_o (measured in centimeters; the analog of stored elastic strain in the chamber at end systole) and recoils from rest (initial velocity = 0, corresponding to no flow before valve opening). These parameters (x_o, c, and k) are determined directly from the clinical E-wave contour. Their physiologic interpretation has been extensively validated using gold-standard (simultaneous micromanometric hemodynamics and echocardiography) methods that causally relate these parameters to chamber properties that determine DF.[23,26,45,46] Its applications in physiology include: generation of the third[47] and fourth heart sounds,[48] constant-volume attribute of the four-chambered heart,[49] physiologic and clinical significance of mitral annular oscillations or longitudinal *ringing* of the ventricle in diastole,[50,51] decomposition of E-wave deceleration time into its stiffness and relaxation components,[52] and determination of the *in-vivo* equilibrium volume of the LV as the volume at diastasis.[53]

References

1. Lauschke J, Maisch B. Athlete's heart or hypertrophic cardiomyopathy? *Clin Res Cardiol*. 2009;98:80–88.
2. Maron BJ, McKenna WJ, Danielson GK, et al. American College of Cardiology/European Society of Cardiology clinical expert consensus document on hypertrophic cardiomyopathy. A report of the American College of Cardiology Foundation Task Force on Clinical Expert Consensus Documents and the European Society of Cardiology Committee for Practice Guidelines. *J Am Coll Cardiol*. 2003;42:1687–1713.
3. Maron BJ, Maron MS. Hypertrophic cardiomyopathy. *Lancet*. 2013;381:242–255.
4. Mone SM, Sanders SP, Colan SD. Control mechanisms for physiological hypertrophy of pregnancy. *Circulation*. 1996;94:667–672.
5. Dickhuth HH, Röcker K, Hipp A, et al. Echocardiographic findings in endurance athletes with hypertrophic non-obstructive cardiomyopathy (HNCM) compared to non-athletes with HNCM and to physiological hypertrophy (athlete's heart). *Int J Sports Med*. 1994;15:273–277.
6. Maron BJ, Pelliccia A, Spirito P. Cardiac disease in young trained athletes. Insights into methods for distinguishing athlete's heart from structural heart disease, with particular emphasis on hypertrophic cardiomyopathy. *Circulation*. 1995;91:1596–1601.
7. Pelliccia A, Maron BJ. Athlete's heart electrocardiogram mimicking hypertrophic cardiomyopathy. *Curr Cardiol Rep*. 2001;3:147–151.
8. Richand V, Lafitte S, Reant P, et al. An ultrasound speckle tracking (two-dimensional strain) analysis of myocardial deformation in professional soccer players compared with healthy subjects and hypertrophic cardiomyopathy. *Am J Cardiol*. 2007;100:128–132.
9. Matsumura Y, Elliott PM, Virdee MS, et al. Left ventricular diastolic function assessed using Doppler tissue imaging in patients with hypertrophic cardiomyopathy: relation to symptoms and exercise capacity. *Heart*. 2002;87:247–251.
10. Severino S, Caso P, Galderisi M, et al. Use of pulsed Doppler tissue imaging to assess regional left ventricular diastolic dysfunction in hypertrophic cardiomyopathy. *Am J Cardiol*. 1998;82:1394–1398.
11. Florescu M, Vinereanu D. How to differentiate athlete's heart from pathological cardiac hypertrophy? *Mædica J Clin Med*. 2006;1:19–26.
12. Galanti G, Toncelli L, Del Furia F, et al. Tissue Doppler imaging can be useful to distinguish pathological from physiological left ventricular hypertrophy: a study in master athletes and mild hypertensive subjects. *Cardiovasc Ultrasound*. 2009;7:48.
13. Lewis JF, Spirito P, Pelliccia A, et al. Usefulness of Doppler echocardiographic assessment of diastolic filling in distinguishing "athlete's heart" from hypertrophic cardiomyopathy. *Br Heart J*. 1992;68:296–300.
14. Briguori C, Betocchi S, Losi MA, et al. Noninvasive evaluation of left ventricular diastolic function in hypertrophic cardiomyopathy. *Am J Cardiol*. 1998;81:180–187.
15. Palazzuoli A, Puccetti L, Bruni F, et al. Diastolic filling in hypertrophied hearts of elite runners: an echo-Doppler study. *Eur Rev Med Pharmacol Sci*. 2001;5:65–69.
16. Fagard R. Athlete's heart. *Heart*. 2003;89:1455–1461.
17. Pavlik G, Olexó Z, Sidó Z, et al. Doppler echocardiographic examinations in the assessment of the athletic heart. *Acta Physiol Hung*. 1999;86:7–22.
18. King GJ, Murphy RT, Almuntaser I, et al. Alterations in myocardial stiffness in elite athletes assessed by a new Doppler index. *Heart*. 2008;94:1323–1325.
19. Paelinck BP, van Eck JW, De Hert SG, et al. Effects of postural changes on cardiac function in healthy subjects. *Eur J Echocardiogr*. 2003;4:196–201.
20. Pepi M, Guazzi M, Maltagliati A, et al. Diastolic ventricular interaction in normal and dilated heart during head-up tilting. *Clin Cardiol*. 2000;23:665–672.
21. Völler H, Uhrig A, Spielberg C, et al. Acute alterations of pre- and afterload: are Doppler-derived diastolic filling patterns able to differentiate the loading condition? *Int J Card Imaging*. 1993;9:231–240.
22. Shmuylovich L, Kovács SJ. E-wave deceleration time may not provide an accurate determination of LV chamber stiffness if LV relaxation/viscoelasticity is unknown. *Am J Physiol Heart Circ Physiol*. 2007;292:H2712–H2720.
23. Kovács Jr SJ, Barzilai B, Pérez JE. Evaluation of diastolic function with Doppler echocardiography: the PDF formalism. *Am J Physiol*. 1987;252:H178–H187.
24. Apor A, Merkely B, Morrell T, et al. Diastolic function in Olympic athletes versus controls: stiffness-based and relaxation-based echocardiographic comparisons. *J Exerc Sci Fit*. 2013;11:29–34.
25. Nagueh SF, Appleton CP, Gillebert TC, et al. Recommendations for the evaluation of left ventricular diastolic function by echocardiography. *J Am Soc Echocardiogr*. 2009;22:107–133.
26. Kovács SJ, Setser R, Hall AF. Left ventricular chamber stiffness from model-based image processing of transmitral Doppler E-waves. *Coron Artery Dis*. 1997;8:179–187.
27. Mosteller RD. Simplified calculation of body-surface area. *N Engl J Med*. 1987;317:1098.
28. Nihoyannopoulos P, Karatasakis G, Frenneaux M, et al. Diastolic function in hypertrophic cardiomyopathy: relation to exercise capacity. *J Am Coll Cardiol*. 1992;19:536–540.
29. Shmuylovich L, Kovács SJ. Load-independent index of diastolic filling: model-based derivation with *in vivo* validation in control and diastolic dysfunction subjects. *J Appl Physiol*. 2006;(101):92–101.
30. Maron BJ. Distinguishing hypertrophic cardiomyopathy from athlete's heart: a clinical problem of increasing magnitude and significance. *Heart*. 2005;91:1380–1382.
31. Gwathmey JK, Warren SE, Briggs GM, et al. Diastolic dysfunction in hypertrophic cardiomyopathy. Effect on active force generation during systole. *J Clin Invest*. 1991;87:1023–1031.

32. Wigle ED. Hypertrophic cardiomyopathy: a 1987 viewpoint. *Circulation*. 1987;75:311−322.
33. Little WC, Ohno M, Kitzman DW, et al. Determination of left ventricular chamber stiffness from the time for deceleration of early left ventricular filling. *Circulation*. 1995;92:1933−1939.
34. Riordan MM, Chung CS, Kovács SJ. Diabetes and diastolic function: stiffness and relaxation from transmitral flow. *Ultrasound Med Biol*. 2005;31:1589−1596.
35. Kovács SJ, Rosado J, Manson McGuire AL, et al. Can transmitral Doppler E-waves differentiate hypertensive hearts from normal? *Hypertension*. 1997;30:788−795.
36. Riordan MM, Weiss EP, Meyer TE, et al. The effects of caloric restriction- and exercise-induced weight loss on left ventricular diastolic function. *Am J Physiol Heart Circ Physiol*. 2008;294:H1174−H1182.
37. Rich MW, Stitziel NO, Kovács SJ. Prognostic value of diastolic filling parameters derived using a novel image processing technique in patients > or = 70 years of age with congestive heart failure. *Am J Cardiol*. 1999;84:82−86.
38. Bauman L, Chung CS, Karamanoglu M, et al. The peak atrioventricular pressure gradient to transmitral flow relation: kinematic model prediction with *in vivo* validation. *J Am Soc Echocardiogr*. 2004;17:839−844.
39. Sanderson JE, Gibson DG, Brown DJ, et al. Left ventricular filling in hypertrophic cardiomyopathy. An angiographic study. *Br Heart J*. 1977;39:661−670.
40. Betocchi S, Hess OM, Losi MA, et al. Regional left ventricular mechanics in hypertrophic cardiomyopathy. *Circulation*. 1993;88:2206−2214.
41. Boardman NT, Aronsen JM, Louch WE, et al. Impaired left ventricular mechanical and energetic function in mice after cardiomyocyte-specific excision of SERCA2. *Am J Physiol Heart Circ Physiol*. 2014;306:H1018−H1024.
42. Ghosh E, Kovács SJ. Early left ventricular diastolic function quantitation using directional impedances. *Ann Biomed Eng*. 2013;41:1269−1278.
43. George KP, Batterham AM, Jones B. The impact of scalar variable and process on athlete-control comparisons of cardiac dimensions. *Med Sci Sports Exerc*. 1998;30:824−830.
44. Batterham AM, George KP, Mullineaux DR. Allometric scaling of left ventricular mass by body dimensions in males and females. *Med Sci Sports Exerc*. 1997;29:181−186.
45. Kovács SJ, Meisner JS, Yellin EL. Modeling of diastole. *Cardiol Clin*. 2000;18:459−487.
46. Lisauskas JB, Singh J, Bowman AW, et al. Chamber properties from transmitral flow: prediction of average and passive left ventricular diastolic stiffness. *J Appl Physiol (1985)*. 2001;91:154−162.
47. Manson AL, Nudelman SP, Hagley MT, et al. Relationship of the third heart sound to transmitral flow velocity deceleration. *Circulation*. 1995;92:388−394.
48. McGuire AM, Hagley MT, Hall AF, et al. Relationship of the fourth heart sound to atrial systolic transmitral flow deceleration. *Am J Physiol*. 1997;272:H1527−H1536.
49. Bowman AW, Kovács SJ. Assessment and consequences of the constant-volume attribute of the four-chambered heart. *Am J Physiol Heart Circ Physiol*. 2003;285:H2027−H2033.
50. Riordan MM, Kovács SJ. Quantitation of mitral annular oscillations and longitudinal "ringing" of the left ventricle: a new window into longitudinal diastolic function. *J Appl Physiol (1985)*. 2006;100:112−119.
51. Riordan MM, Kovács SJ. Absence of diastolic mitral annular oscillations is a marker for relaxation-related diastolic dysfunction. *Am J Physiol Heart Circ Physiol*. 2007;292:H2952−H2958.
52. Mossahebi S, Kovács SJ. Kinematic modeling based decomposition of transmitral flow (Doppler E-wave) deceleration time into stiffness and relaxation components. *Cardiovasc Eng Technol*. 2014;5(1):25−34.
53. Shmuylovich L, Chung CS, Kovács SJ. Last word on point: counterpoint: left ventricular volume during diastasis is the physiological *in vivo* equilibrium volume and is related to diastolic suction. *J Appl Physiol (1985)*. 2010;109(2):615.